INTERNATIONAL JOURNAL OF ENVIRONMENT

Volume-11, Issue-2, 2022 ISSN 2091-2854

Received: 21 April 2022 *Revised: 2 July 2022* *Accepted: 19 July 2022*

ESTIMATION OF SURFACE $PM_{2.5}$ WITH MODIS AEROSOL OPTICAL DEPTH AND SOURCE IDENTIFICATION USING TRAJECTORY ANALYSIS: A CASE OF HYDERABAD CITY, INDIA

Selvetikar Ashok[1]*, M Chandra Sekhar[2] and D Rama Bhupal Reddy[3]

[1,2]Department of civil engineering, National Institute of Technology Warangal-506004, Telangana, India

[3]Department of civil engineering GMR Institute of Technology, GMR Nagar-532127, AP, India

*Corresponding author: sashok007@student.nitw.ac.in

Abstract

Satellite measurements are important for quantifying the ground observations and atmosphere columnar properties like Aerosol Optical Depth (AOD) especially in developing countries like India. In this study Moderate Resolution Imaging Spectroradiometer (MODIS) retrieval's AOD product has been used having 3 km and 10 km spatial resolution from terra and aqua satellites, The MODIS AOD data and meteorological parameters from May 2017 to May 2019 were used. The Multiple linear regression method is implemented in this study. The study concluded that there is a good agreement in the prediction of $PM_{2.5}$ at Zoopark location, whereas in other monitoring locations the agreement between AOD and measured $PM_{2.5}$ is relatively poor. The particulate matter (PM) concentrations are influenced by the local source regions and the long-range transport of pollutant through the wind, whereas the source regions identified based on the Potential Source Contribution Function (PSCF), Concentration-Weighted Trajectory (CWT) and Cluster analysis indicate the dominant source regions. Results indicate that the Central India and East Indian regions are more dominating source regions at Hyderabad location in the winter season. It was found that the lower altitude layer showed the major source of local regions nearby receptor. The cluster analysis indicates that the high intensity from the East Indian regions. This paper not only demonstrates reasonable prediction accuracy but also provides the model uncertainties which lays foundation for further study.

Keywords: MODIS, CWT, PSCF, Cluster analysis

DOI: https://doi.org/10.3126/ije.v11i2.44538

1. Introduction

The PM particles study is important because of its relevance on environment and public health (Harrison and Yin, 2000). Exposure to PM causes major diseases such as cardiopulmonary diseases (Newman et al., 2020), preterm birth (8%) and low birth weight (28%) (Bachwenkizi et al., 2022), carcinogenicity (Abba et al., 2012), lung cancer (Raaschou-Nielsen et al., 2016). The majority of these deaths are from ambient particulate matter pollution (Pandey et al., 2021). However, the urbanization and population growth was one of the parameter for the increments in PM levels (Sharma and Maloo, 2005). The number of continuous monitoring stations are limited in India and the spatial distribution also matters in the urban air quality monitoring studies. Hence, monitoring $PM_{2.5}$ across urban and rural regions of India is challenging. The city-scale monitoring stations are crucial for the categorization of city pollution and the ability to accurately assess the health impact. However, the daily PM data is mandatory for the health impact study. The missing PM data can be predicted using satellite AOD and meteorological data. The daily $PM_{2.5}$ maps are useful to identify pollution "hotspots" and estimate short- and long-term exposure.

The satellite AOD retrievals and PM prediction are well discussed in literature (Ferrero et al., 2019; Pant et al., 2016). AOD represents the columnar property of aerosol and the PM represent the surface loading of the aerosol. The relation between AOD and PM is studied by researchers using different types of models (Lee et al., 2011; Yap and Hashim, 2013; You et al., 2015; Park et al., 2020; Yang et al., 2019). Soni et al. (2018) reported that log-linear regression models are better performing in Jaipur region. In the current study multiple linear regression model was adopted. Furthermore, studies also considered relative humidity (RH) (Ma et al., 2019), Temperature (T) and Boundary layer height (Chu et al., 2015; Liu et al., 2005), Visibility (Ying et al., 2004), and reduction in solar radiation (SR) (Kumar et al., 2019) for assessing the influence of PM concentration on meteorology. Koelemeijer et al. (2006) considered the height of planetary boundary layer (HPBL) and relative humidity in prediction of $PM_{2.5}$. Later, Tian and Chen, (2010) concluded that the temperature and RH were more important than HPBL for prediction of PM. The current study did not consider HPBL. Studies reported use of different AOD satellites to predict the PM at ground level with high resolution (10x10,1^{o}x1^{o}) (Kharol et al., 2011; Tuna Tuygun et al., 2021).Very few studies are available on MODIS aqua and terra AOD prediction of $PM_{2.5}$ at fine resolution. In this study, fine resolution (3x3km) AOD and meteorological parameters are considered for prediction of $PM_{2.5}$. The $PM_{2.5}$ concentrations have great influence on source nature and strength, as well as the meteorological parameters in the study region. However, the receptor models are used to indicate relation between source and receptor. Most of the researchers used the Chemical mass balance (CMB), Positive matrix factorization model (PMF) and Principal Component Analysis (PCA) analysis (Jain et al., 2021; Kalaiarasan et al., 2018) for PM prediction. The ensemble trajectory techniques produce qualitative analysis of predominant transportation paths.

Wind speed and direction are the predominant parameters in transportation of aerosols (Das et al., 2021). Sun et al. (2001) studied transport of aerosol dust from far away regions through the elevated layers (<3000m) towards the receptor regions. Biomass burning significantly affected the aerosol optical properties locally as well in the downwind regions (Shaik et al., 2019). The overall aerosol properties change based on their production mechanisms, removal and transport processes (Ramachandran et al., 2012). Receptor models are very popular while trajectory based models are not that popular in India (Banerjee et al., 2015). The long-range trajectory transport of pollutants indicated the influence of anthropogenic pollution (Ramachandran, 2005). The Trajectory based study by Shaik et al. (2019) revealed that the transport pathways at receptor location.

The ground level $PM_{2.5}$ was measured at fixed locations but its representation of spatial coverage was limited. Spatial interpolation methods like kriging (Ma et al., 2014) and nearest-neighbor (Just et al., 2015) are used. However, the spatial interpolation leads to uncertainties due to limited ground monitoring stations and uneven distribution of stations in urban regions. To address these challenges, establishing correlation with the satellite MODIS AOD product and $PM_{2.5}$ was attempted in study region. Receptor models demonstrate strong interaction with in the source and receptor (Pant and Harrison, 2012). To establish the relationship with the source and receptor location, the back trajectory model was adopted in this study, as no such studies are reported for this region with complex land uses like industrial, residential, commercial and high-rise buildings. It was necessary to understand the variations in $PM_{2.5}$ concentrations and source identification. For identification of ground level $PM_{2.5}$, MODIS instrument Terra/Aqua AOD and meteorological parameters are used in the present study. MLR and back trajectory analysis are also attempted to find potential source regions contributing $PM_{2.5}$ by long range transport. The study will be a utility tool to predict air quality economically using the MODIS AOD when air quality monitoring is difficult in large regions.

2. Methodology

2.1 Study area

Hyderabad City located in South India (17°12' to 17°6' N and 78°66' to 78°70'E; 540 MSL), with population over 8 million is the state capital of Telangana. The total area city covered nearly 650 km^2, the average annual rainfall of the city is 840 mm during 1991–2013 (Agilan and Umamahesh, 2015). The Central Pollution Control Board (CPCB) monitoring points are shown in Fig. 1. The study region is dominate by transportation, industrial, commercial and residential land uses with mixed land uses as well. Seasonal climate prevails in the study area with hot summer (March-June), cold winters (November to February) and rains during monsoon season (July to October) (Kumar et al., 2017). The Hyderabad $PM_{2.5}$ annual average is 56μg m^{-3}peaking during the winter morning rush hours (140μg m^{-3}) (Chen et al., 2020). The MODIS level 3 dataset

AOD range from 0.15 up to 0.5 and observed relatively good correlation with AOD (0.6-0.7) (Kharol et al., 2011). Gummeneni et al., (2011), identified dominating pollution activities: vehicular (31%) and resuspended dust (26%). The study by Guttikunda and Aggarwal, (2009) reveled traffic sources dominating 50% of the total pollution. The long range pollutant from Thar Desert was reported by Badarinath et al. (2007). The contributions of local and long-range pollutants are dominating the study region.

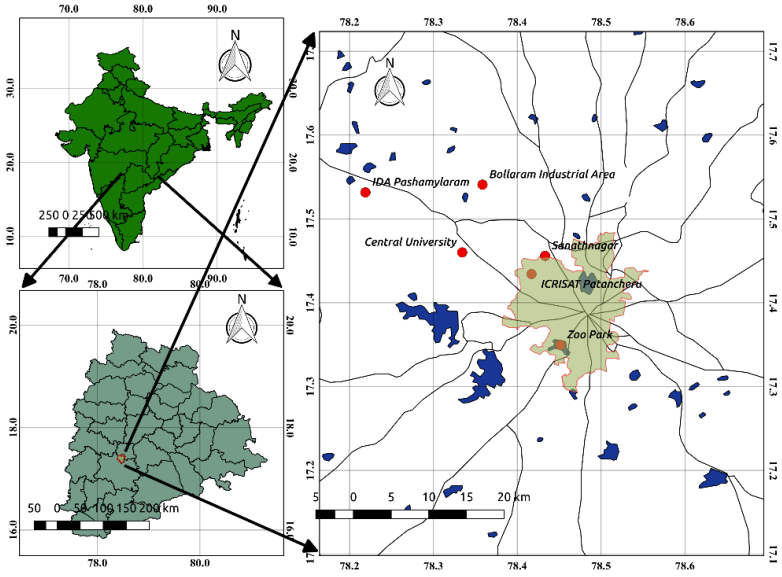

Fig. 1. Study location Hyderabad (six locations)

2.2. Data collection

2.2.1. MODIS instrument AOD: The satellite AOD dataset provided by the Moderate Resolution Imaging Spectroradiometer (MODIS) on the Terra/Aqua instrument (Remer et al., 2005) was used in the present study. The MODIS instrument produces global coverage in 1 or 2 days. In this study, AOD data from Terra (MOD04_3K, MOD04_L2) and Aqua (MYD04_3K, MYD04_L2) are used, which is reported 3K for 3Km and L2 for 10km The MODIS AOD data product was downloaded from NASA LAADS (https://ladsweb.modaps.eosdis.nasa.gov/). The southward Terra crosses about 10:30 Local Solar Time (LST), whereas, Aqua northward about 13:30 LST. The time difference between Terra and Aqua are approximately 1.5h and 4.5h in the northern Hemisphere and the southern Hemisphere respectively (Kaufman et al., 2005), The time interval for Hyderabad was 2.5h (Kharol et al., 2011). MODIS measures AOD with an estimated uncertainty of 0.05 AOD±0.15 for Level 2 over land (Remer et al., 2005) at 0.47and 0.66mm extrapolated at 0.55mm (Ichoku, 2002). The two separate algorithms described in literature over land and ocean surfaces are adopted (Kaufman and Tanré, 1998).

The Dark Target (DT) aerosol algorithm is used to create a new 3 km aerosol product (Levy et al., 2017). In this study to match overpass time of Terra/Aqua satellite in the region of Hyderabad, respective $PM_{2.5}$ average concentrations at study locations available from the CPCB monitoring points over Hyderabad

region were used. Data was extracted from HDF files with help of Python scripts for corresponding latitude and longitude of all locations. The CPCB motoring points located with nearest point in data entered location (haversine formula) of the each HDF file (Gupta and Follette-Cook, 2020). AOD single grid (3x3 or 5x5) data was used for missing data. The high AOD values represent higher pollution, cloud contamination and dust storm on the study region. To avoid uncertainties in AOD, higher values above 1 AOD were excluded in this study.

2.2.2. Meteorological data: The meteorological data was obtained from CPCB (https://app.cpcbccr.com/ccr/#/caaqm-dashboard-all/caaqm-landing) monitoring locations over Hyderabad. The meteorological parameters Temperature (AT), Relative Humidity, pressure (BP), Solar Radiation (SR), wind speed (WS) and direction (WD) and $PM_{2.5}$ data collected over the period of May 2017 to May 2019 (two years) was used in the study. For further analysis, flow chart in Fig. 2, gives details of the methodology adopted in the study for identification of source regions at receptor location.

2.2.3. Multiple linear regression model: The multiple linear regression was established with in the $PM_{2.5}$ and MODIS AOD along with meteorological parameters, the MLR shown in Eq.1. However, b0 represent the model intercept and the b1, b2, ..., b7, represent the model parameters to be estimated. The **ε** represent error term that individual outcomes will vary about that mean. The assumption was error terms are normally distributed and homoscedastic, that is, the variance of the errors is the same across all levels of the independent variables. The best fit location identified based on MLR, later the location latitude and longitude were used in the Hybrid Single-Particle Lagrangian Integrated Trajectory model (HYSPLIT) model for back trajectory analysis.

$$PM_{2.5} = b_0 + b_1(AOD) + b_2(AT) + b_3(RH) + b_4(WS) + b_5(WD) + b_6(SR) + b_7(BP) + \varepsilon \ldots \text{Eq.1}$$

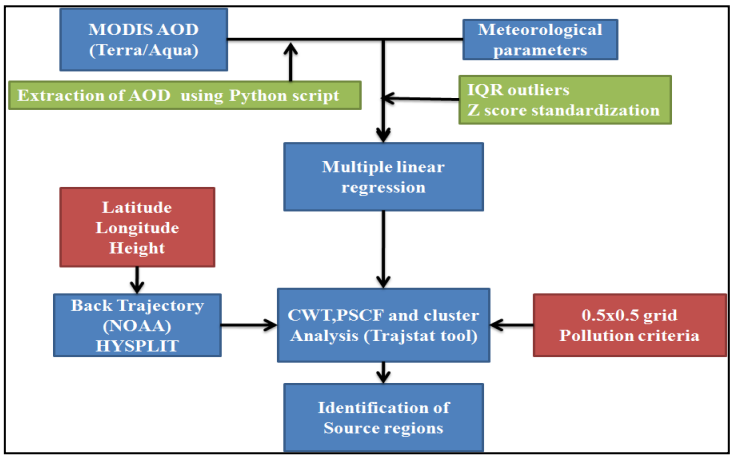

Fig. 2. Study flow chart for identification of source region

2.2.3. Backward trajectory: The Back trajectory data collected from Global Data Assimilation System (GDAS), the U.S. National Oceanic and Atmospheric Administration (NOAA) (Wang et al., 2009) was used. The 7-day back trajectories at a height (100, 500 and 1000m) was considered as surface layer and elevated

layer (1500 and 2000m) for source analysis. The back trajectories require sophisticated computations of transport, chemical transformation, and deposition of pollutants and hazardous materials (Draxler and Hess., 1998).

2.2.4. CWT analysis: The spatial resolution 0.5×0.5° was used to find the source paths. The Concentrated Weighted Trajectory (CWT) value indicates the source strength (Cheng et al., 2013). The number of trajectory segment endpoints that end with in a grid cell will give PSCF value of the corresponding grid (Han et al., 2007). In the CWT method, each grid cell is assigned a weighted concentration by averaging the sample concentration (Seibert et al., 1994). The trajectory endpoint time in the grid cells have been weighted by $PM_{2.5}$ corresponding trajectory. Concentration of each grid cell calculated based on below Eq.2 (Chen et al., 2018).

$$CWT_{ij} = \frac{\sum_{l=1}^{L} c_l \tau_{ijL}}{\sum_{l=1}^{L} c_l \tau_{ijl}} \ldots\ldots..\text{Eq.2}$$

C_l is the predicted mean concentration of a $PM_{2.5}$; l denote the associated backward trajectory; τijl each segment endpoints in 0.5x0.5 grid cells (i, j); L presents the total number of backward trajectories consider in this study.

2.2.5. PSCF analysis

The Potential Source Contribution Function (PSCF) shown in Eq.3, defines the probability that a receptor area impacted from identified regions. Negral et al. (2020) reported studies on identification of sources using PSCF. Liao et al. (2017) used PSCF for identification of pollutants in China during the winter season. The 24hour average standards for $PM_{2.5}$ concentration (60μg m^{-3}) in ambient air quality standards of India, it was adopted from the studies by Li et al. (2020); Liao et al. (2017). The same criteria adopted in the present study. Grid cells with greater than the 60μg m^{-3} fall within the ijth grid cell (Zhang et al., 2015).

$$PSCF_{ij} = \frac{M_{ij}}{N_{ij}} W_{ij} \ldots\ldots. \text{Eq.3}$$

Where, M_{ij} represent the total number of back trajectories with each grid cell (i, j), N_{ij} present the total number of back trajectories with respective each grid cell (i, j); Wij denote weighting function of back trajectory segment endpoints in a grid cell (i, j) (Fu et al., 2012).

2.2.6. Cluster Analysis: The K-mean cluster technique is extensively used air mass trajectories to represent the pollutant pathways (Govender and Sivakumar, 2020). In the present study, k-mean cluster was adopted for clustering the back trajectories. The clustering technique shows the average trajectory paths for each cluster.

The present study divided in to two parts, firstly prediction of $PM_{2.5}$ based on meteorology and MODIS AOD. Second part attempts back trajectory analysis to identify the potential source regions. During the study, data outliers are removed from the secondary data obtained from CPCB and subsequently Z-score parameter was used for standardization of data. The filtered data divided into 80% for model development and 20% for model

validation. Statistical parameters (RMSE, NMB, d and R) were used to identify the best fit location. Sathe et al. (2019) used statistical analysis for his study as well. Furthermore, the source identification based on CWT, PSCF and Cluster analysis was carried out. GIS based software MeteoInfo tool was used for meteorological data visualization and analysis (Wang, 2014). The PSCF, CWT and Cluster analysis were analyzed using plugin TrajStat tool (Wang et al., 2009). Four seasons (Winter, Pre-monsoon, Monsoon and Post-monsoon) were considered during the study for source analysis.

3. Results and discussion

3.1. Variation of meteorological parameters

The presence of particulates in the atmosphere will be reflected by AOD, the intensity of the light received by the instrument will shows as columnar property of atmosphere. Satellite-based AOD measurements have been widely used to predict the $PM_{2.5}$ and PM_{10} (Shao et al., 2017; Soni et al., 2018). The mean AOD obtained during the study are shown in Fig. 3. The mean AOD variation at Bollarm (0.54±0.21), Central University (0.54±0.23), IDA (0.50±0.2), Patancheru (0.55±0.23) Sanathnagar (0.52±21) and Zoopark (0.47±0.22). High AOD was observed at Patancher and the least AOD at Zoopark location. Higher AOD values at Patancher is perhaps due to concentrated industrial activity while Zoopark represents minimum anthropogenic activity. Soni et al. (2018) reported average AOD as 0.42 and the range as 0.02–1.67 in Jaipur region. AOD values were higher during the pre-monsoon and winter with a subsequent decrease in the summer period. Similar results are reported by Pani and Verma, (2014). The temperature and relative humidity values are comparable to those reported in the Jaipur region reported by Soni et al. (2018). Temperature inversion leads to higher values of pollutants in the winter season at ground level (Yadav et al., 2019). The wind speed and direction are also important parameters in the dispersion and transport of particles. These particles move along with the wind from one region to faraway regions depending on strength of wind and atmospheric stability conditions. Hence, the meteorological parameters crucial for the identification of the particulate concentration at the receptor location (Das et al., 2021; Y. Zhang et al., 2017). The influence of climate change on particulate pollution and trans-boundary aerosols was reported by Deb and Sil. (2019); Tiwari et al. (2015); Yadav et al. (2016). Fig. 3, shows the meteorology, $PM_{2.5}$ and AOD of the six locations with standard deviations. Higher variations are observed in BP and SR at all locations. Lower deviations in AT, RH, PM and AOD are observed. This is perhaps due to the topography of land and climatic conditions. In the present study, the higher mean temperature was observed at the Patancher area (30.51^{o}C) may be due to the industrial zone.

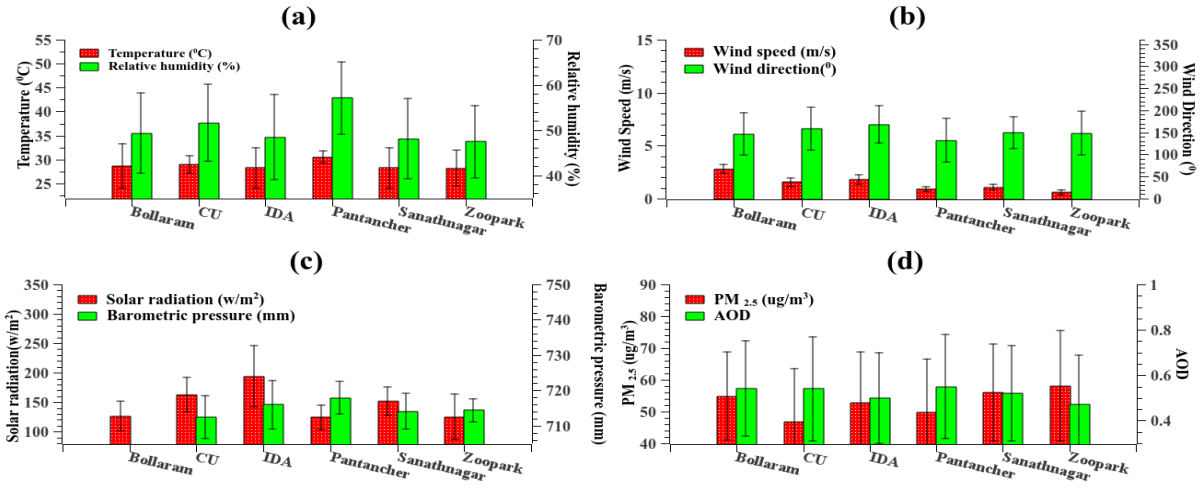

Fig. 3. Meteorological variation of all locations (a) RH(%) and Temperature(^{0}C), (b) Wind speed (m s^{-1}) and Wind direction (degrees) (c) Barometric pressure(mm) and Solar radiation(Wm^{-2}) (d) $PM_{2.5}$ (µg m^{-3}) and AOD

3.2. MODIS AOD for prediction of the $PM_{2.5}$

The MODIS (MOD_3K, MOD_L2, MYOD_3K and MYOD_L2) product was used in the current study. The AOD- $PM_{2.5}$ relation is highly accurate in some locations in India (Chelani, 2018). In coastal areas $PM_{2.5}$-AOD relation was weaker (Yang et al., 2019). Few studies indicated positive and weaker correlation with in the AOD- $PM_{2.5}$ (Chelani, 2018; Yang et al., 2019). However, in the present study positive correlation was established with in AOD- $PM_{2.5}$ at some locations.

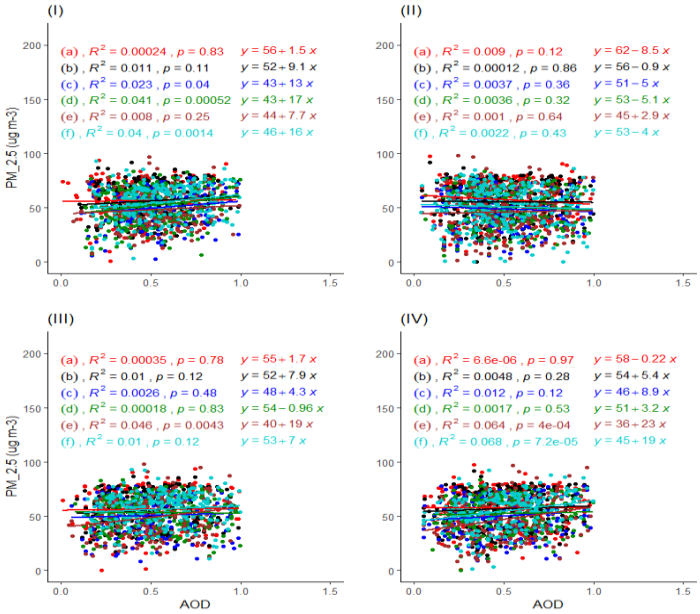

Fig. 4. AOD- $PM_{2.5}$ correlation with in MODIS product at all locations, (I) MOD_3K(3km), (II) MOD_L2(10km), (III) MYOD_3K(3km), (IV) MYOD_L2(10km), (a) Zoopark, (b) Sanathnagar, (c) Patancher, (d) IDA, (e) Central Univercity(CU, (f) Bollaram.

The linear regression results between AOD- $PM_{2.5}$ are presented in Fig. 4. Results indicate weak positive correlation in some locations with relatively higher correlation at Bollaram. Single grid of each pixel was chosen for the study, the missing AOD data was replaced with average AOD of 3x3 or 5x5 grid. The variations are perhaps due to the urban conditions and geographical differences. Local dominating sources also result in variations.

Multiple regression analysis of AOD and metrological parameters was used to obtain ground level PM 2.5 concentration. Statistical parameters (R, RMSE, d and NMB) for the six locations are presented in Table A1. Results indicted relatively good agreement at Zoopark when compared to other five locations. The scatter plots for observed and predicted concentrations (for 10km resolution of aqua and terra product) are presented in Fig. 5. Earlier studies reported similar correlation coefficients (0.30 to 0.46) between Level 3 Terra/Aqua MODIS and MICROTOPS-II,AOD550 in all seasons (Kharol et al., 2011).

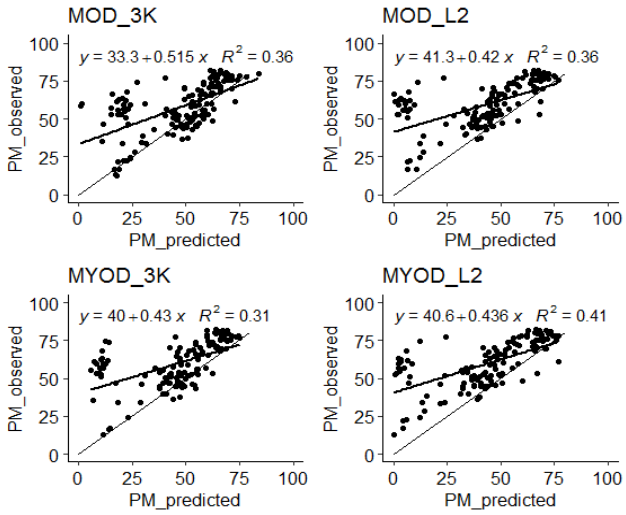

Fig. 5. Scatter plot for $PM_{2.5}$ Predicted and Observed at Zoopark location for four MODIS AOD product.

Shao et al. (2017) in his studies on AOD-$PM_{2.5}$ in Nanjing of the Yangtze River Delta, concluded that there was a high consistency of AOD versus $PM_{2.5}$ and the correlation coefficient was (R^2) 0.56. In the current study, the values are slightly lower around 0.4. Variations in MODIS are generally caused by deserts (Sathe et al., 2019) and cloud properties (Gopal et al., 2016).

The MOD_3K product has negative Normalized Mean Bias (NMB) except for Zoopark location. The correlation coefficients were higher for Zoopark, IDA and Sanathnagar; lower values for Patancheru, Bollarm and CU regions. RMSE was higher (54µg m^{-3}) at Patancher and low for other locations (11-15µg m^{-3}). RMSE values at Patancher peaked in all MODIS collection when compared with other locations. The MOD_L2 results indicated over-prediction at CU and Zoopark locations, while under prediction was observed for other

locations. The correlation was higher (0.41) at the Zoopark while correlation was low at Patancheru. The RMSE variation range (11-14μg m^{-3}) except the Patancheru region. The MYOD_3K and MYOD_L2 have nearly similar values in RMSE, d and NMB indicating good agreement in correlation coefficient in MYOD_3K product. Greater resolution data resulted in higher deviation from the standard line in this study. Kumar et al. (2008) reported that the finer resolution of MODIS_AOD in addition to RH and atmospheric pressure results in better correlation for prediction of $PM_{2.5}$ in New Delhi. The terra AOD product performed better than the aqua in the present study while 10km resolution data performed better than the 3km resolution data in the correlation analysis. Similar results were reported by Wang et al. (2019).

MODIS AOD product obtained for 10km and 3 km resolution is used. The quality of 3 km resolution was generating relatively high noise influencing accuracy of prediction. Munchak et al. (2013) also reported similar observation. The study considered linear relationship between $PM_{2.5}$ and meteorological parameters while the $PM_{2.5}$ formation mechanisms are not considered. The model accuracies are influenced by $PM_{2.5}$ formation mechanism, spatiotemporal heterogeneities and geographical region.

3.3. Back Trajectory analysis for source identification

The MLR analysis was shown that the Zoo Park location was best fit model for prediction of $PM_{2.5}$. Hence, that the Zoo Park location latitude and longitude has been considered for the back trajectory analysis. Local sources and long range transport of pollutants significantly affect the PM 2.5 at receptor location (Mahapatra et al., 2018). The crop residue burning dominant source at Indo Gangetic Plain (IGP) region, India (Ravindra et al., 2019). However, studies on the source identification based on trajectory are limited in India (Banerjee et al., 2015). This study demonstrates indications of probable sources for Hyderabad region. Previous studies also reported results of back trajectory analysis and effective origin source regions and long-range transport of pollutants (Conte et al., 2020; Hong et al., 2019).

3.3.1. Concentration-Weighted Trajectory (CWT):

The CWT analysis for all seasons with in the surface layer presented in Fig. 6(a, b, c, d) and elevated layers in Fig. A1 (d, e, f, g) (Fig. A1 shown in appendix). Results indicate the dominant concentrated paths in the winter season for both surface and elevated layers. The significant trajectory paths were seen from East Indian regions and coastal regions as major source paths for receptor location in winter. During the other seasons, weightage of trajectory is low. Two pathways, one from Central India and the second from Bay of Bengal are identified in pre-monsoon season. During the monsoon, trajectory from West India and Arabian Sea was observed to dominate. Trajectory from East India was observed in post-monsoon region. For surface layer, two pathways dominate in winter and pre-monsoon while one pathway dominated in the other two

seasons. Gebhart et al. (2011) implemented back trajectory for source identification of airborne sulphur and nitrogen. Dust outbreaks were identified using back trajectory in Spain (Cabello et al., 2016). Trajectory analysis was carried out for tracking hazardous air pollution from refinery fire (Shie and Chan, 2013). Comparative studies for source identification were attempted by Kong et al. (2013).

In elevated layer, dominating paths are observed to be from Central India and East India for winter season. During the pre-monsoon the dominating path was from Central India while for post- monsoon, the dominating trajectories were from East India. For monsoon season, trajectories from West India and Arabian Sea dominated. Trajectories from Central India and East India were observed for both surface and elevated layers. Similar trajectories paths were observed in winter and post monsoon for surface and elevated layers while there were differences in the other seasons.

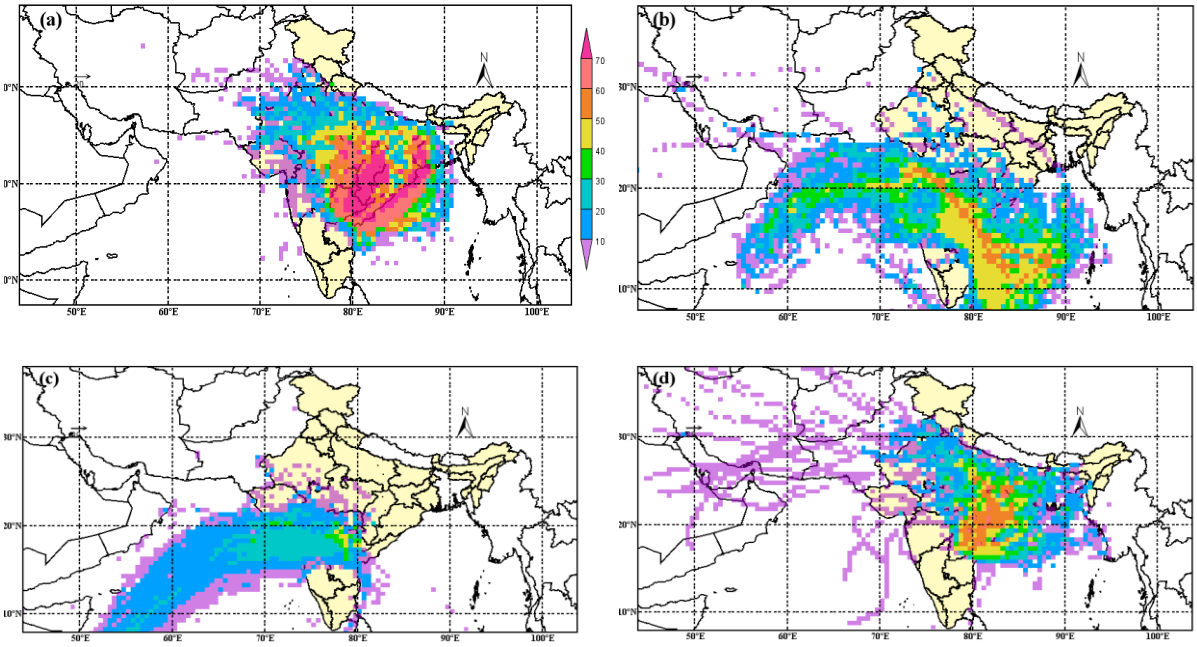

Fig. 6. CWT analysis with different seasons at surface layer [same scale for all figures follows the figure (a) legend].

3.3.2. Potential Source Contribution Function (PSCF):

The potential source contribution function shows the significance regions affecting the receptor location. PSCF (surface layer) for all four seasons in the study region is presented in Fig. 7 (I, II, III and IV). Fig. A2 (shown in appendix) for the elevated layer. For winter season, sources were observed to be from coastal and East direction. In the pre-monsoon, high contributions are from sea regions and from the West region. In this study, it is observed that the long-range transport of pollutants was very less in monsoon and post-monsoon seasons.

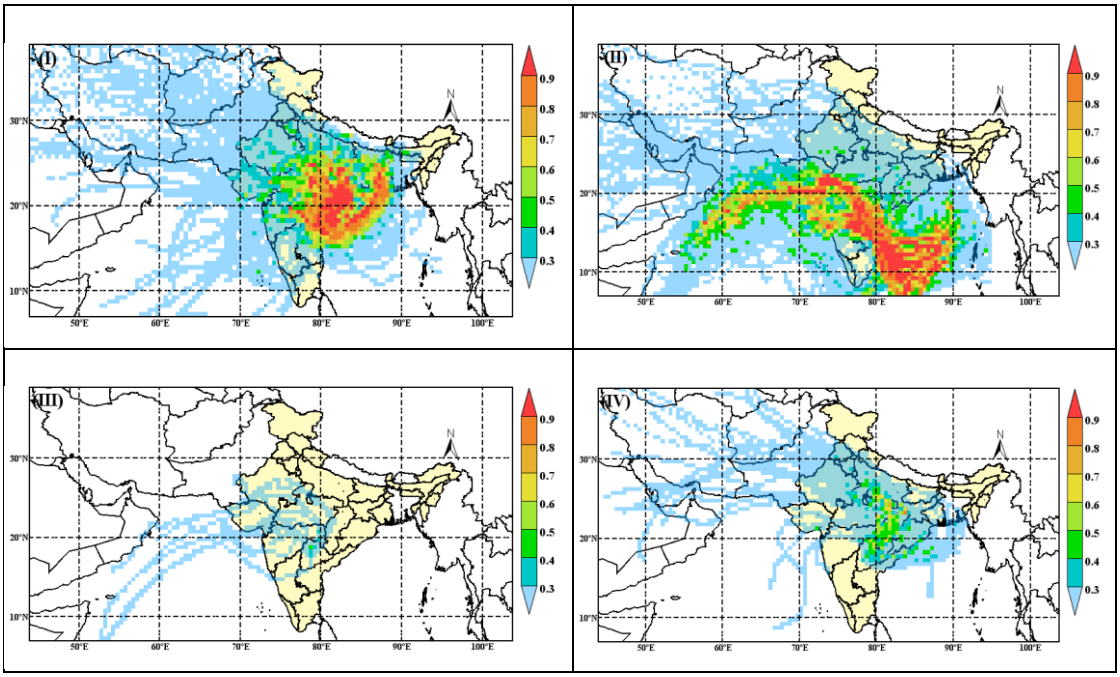

Fig. 7. PSCF analysis with different seasons at surface layer

For the elevated layer, pollutants were dominating from East India regions in the winter season while the contributions are relatively lower for the other three seasons. The CWT and PSCF indicate the dominating paths and source regions. Dust contribution sources were identified from trajectory approach by Wang et al. (2006). The pollutants were observed to travel from far away regions to receptor locations (Jeong et al., 2017).

3.3.3. Cluster analysis: Trajectory cluster analysis was applied to identify the cluster of each seasonal trajectory at receptor location. Fig. 8 (a, b, c and d) shows the winter, pre-monsoon, monsoon and post-monsoon seasons at surface layer and Fig. A3 (e, f, g and h) (Fig. A3 shown in appendix) for elevated layer. The legend shows the heights of the trajectory with respective clusters. Based on direction six clusters were identified for the study. The surface layer clusters are dominating Central India and North West Indian regions in the winter season. The pre-monsoon season has the different direction clusters but the Bay of Bengal has the low-level trajectories. In the monsoon season, clusters from the Arabian Sea region and West India were observed. Most of the trajectories were from local regions in India for surface layer while the trajectories were from outside India for elevated layer. The elevated layer clusters are from for away regions indicating long range transport. For the winter season, three clusters were from high altitudes, while the monsoon season yielded low altitude clusters. The remaining clusters were moderate in altitude.

Surface level trajectory cluster analysis is shown in Table A2 (Table A2 shown in Appendix). Winter_sl polluted cluster was Cluster I with mean concentration as 72.05μg m^{-3} and the number of polluted

trajectories was 179. Highest number of trajectories were observed in Winter_sl season. The least polluted trajectory means as 34.64µg m^{-3}associated with cluster III in monsoon.

The elevated layer cluster analysis is shown in Table A3 (Table A3 shown in Appendix). The highest polluted mean value cluster was cluster II in the winter_el season (71.09µg m^{-3}), while least mean observed in monsoon season was (30.89µg m^{-3}). The pre and post-monsoon season's means were moderate in range 50.95µg m^{-3} and 58.26µg m^{-3} respectively. The polluted clusters have a smaller number of trajectories but the intensity of pollutant transport was more, compared to other clusters.

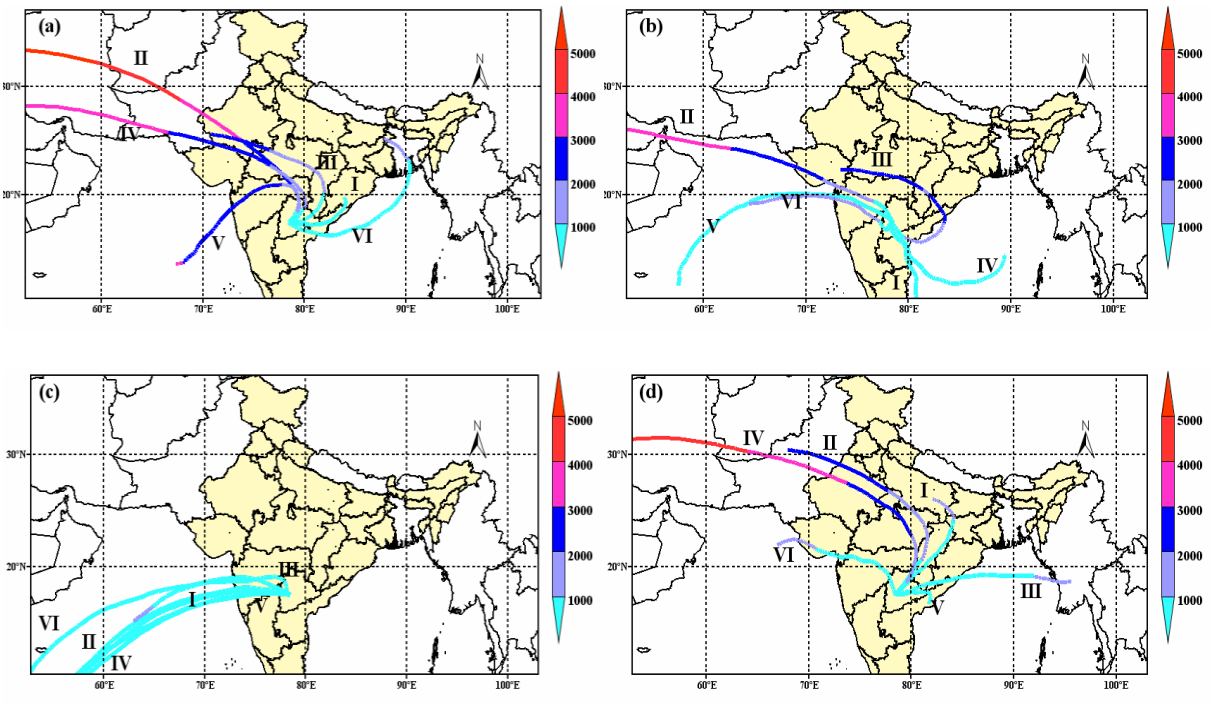

Fig. 8. Cluster analysis with four seasons at surface layer

3.4. Wind rose pattern over Hyderabad region

The wind rose diagrams shown in Fig. 9, indicate wind direction in the study area. The dominating wind direction was from the SE and SW direction at the Zoopark location in autumn season. The mean and standard deviation of wind speed at Zoopark were in the range of 0.78±0.7. The observations from the wind rose and back trajectory analysis indicate similar patterns in the wind direction for the study area. The back trajectory gives the air mass transport from faraway regions. For the other locations, the wind roses are presented in the research results section; Sanathnagar (Fig. A4), Patancher (Fig. A5), IDA (Fig. A6), Central University (Fig. A7), Bollaram (Fig. A8). The mean and standard deviation of wind speed were observed as Sanathnagar (1.25±0.5), Patancher (1.26±0.7), IDA (2.1±0.9), Central University (1.6±0.6), Bollaram (2.6±1.9).

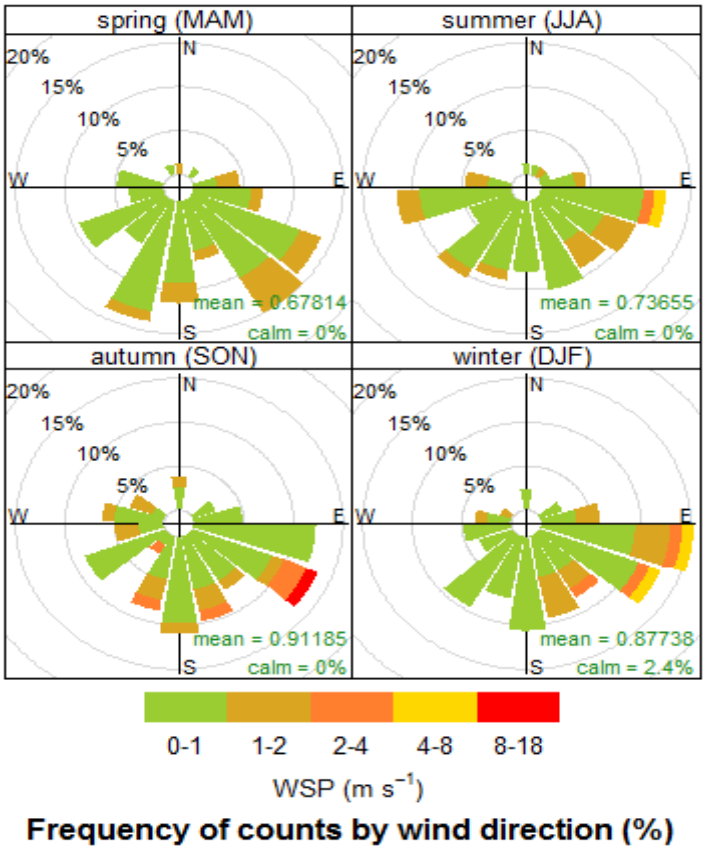

Fig. 9. Zoopark wind rose diagram for all seasons.

4. Conclusion

In this study, assessment of ground-level $PM_{2.5}$ based on multiple regression analysis with the meteorology and retrieved MODIS AOD was attempted. The study suggested that the MODIS terra AOD product seen the best fit for the perdition of $PM_{2.5}$ at Zoo Park location among the six locations. Source identification based on trajectory-based analysis was attempted through CWT, PSCF and cluster analysis. The study identified the long-range transport of the $PM_{2.5}$ and potential source regions contributing to $PM_{2.5}$. East India and Coastal regions were the potential source regions at receptor locations in the winter season. Biomass burning and anthropogenic activities from potential source regions contribute to $PM_{2.5}$ at the receptor location. The cluster analysis provided the main mechanism of transporting paths towards the receptor location. The wind rose pattern identified the local source regions at receptor location. The high $PM_{2.5}$ aerosol mass concentration in Hyderabad City is a reflection of the high emission of local sources such as vehicular transport and anthropogenic activities in addition to long range transport as well. The dominating long range transport pollution at surface layer was observed in winter from East Coastal regions.

Authors' Contribution Statement

SA: Conceptualization, Data collection, Data analysis, Literature review, and Manuscript preparation; MCS:

Supervision, Review, Proofreading, and Editing; DRBR: Data analysis, Literature review, and Manuscript preparation.

Conflict of interest

The authors declare that there are no conflicts of interest regarding the publication of this paper.

Acknowledgments

The authors gratefully acknowledge the NOAA Air Resources Laboratory (ARL) for the provision of the HYSPLIT transport and dispersion model and/or READY website (https://www.ready.noaa.gov) used in this publication

References

Abba, E. J., Unnikrishnan, S., Kumar, R., Yeole, B., and Chowdhury, Z., 2012. Fine aerosol and PAH carcinogenicity estimation in outdoor environment of Mumbai City, India. *International Journal of Environmental Health Research*, *22*(2), 134–149. https://doi.org/10.1080/09603123.2011.613112

Agilan, V., and Umamahesh, N. V., 2015. Detection and attribution of non-stationarity in intensity and frequency of daily and 4-h extreme rainfall of Hyderabad, India. *Journal of Hydrology*, *530*, 677–697. https://doi.org/10.1016/j.jhydrol.2015.10.028

Bachwenkizi, J., Liu, C., Meng, X., Zhang, L., Wang, W., van Donkelaar, A., Martin, R. V., Hammer, M. S., Chen, R., and Kan, H., 2022. Maternal exposure to fine particulate matter and preterm birth and low birth weight in Africa. *Environment International*, *160*, 107053. https://doi.org/10.1016/j.envint.2021.107053

Badarinath, K. V. S., Kharol, S. K., Kaskaoutis, D. G., and Kambezidis, H. D., 2007. Case study of a dust storm over Hyderabad area, India: Its impact on solar radiation using satellite data and ground measurements. *Science of The Total Environment*, *384*(1–3), 316–332. https://doi.org/10.1016/j.scitotenv.2007.05.031

Banerjee, T., Murari, V., Kumar, M., and Raju, M. P., 2015. Source apportionment of airborne particulates through receptor modeling: Indian scenario. *Atmospheric Research*, *164–165*, 167–187. https://doi.org/10.1016/j.atmosres.2015.04.017

Cabello, M., Orza, J. A. G., Dueñas, C., Liger, E., Gordo, E., and Cañete, S., 2016. Back-trajectory analysis of African dust outbreaks at a coastal city in southern Spain: Selection of starting heights and assessment of African and concurrent Mediterranean contributions. *Atmospheric Environment*, *140*, 10–21. https://doi.org/10.1016/j.atmosenv.2016.05.047

Chelani, A. B., 2018. Estimating $PM_{2.5}$ concentration from satellite derived aerosol optical depth and meteorological variables using a combination model. *Atmospheric Pollution Research*, *10*(3), 847–857. https://doi.org/10.1016/j.apr.2018.12.013

Chen, G., Li, S., Knibbs, L. D., Hamm, N. A. S., Cao, W., Li, T., Guo, J., Ren, H., Abramson, M. J., and Guo, Y., 2018. A machine learning method to estimate $PM_{2.5}$ concentrations across China with remote sensing, meteorological and land use information. *Science of The Total Environment*, *636*, 52–60. https://doi.org/10.1016/j.scitotenv.2018.04.251

Chen, Y., Wild, O., Conibear, L., Ran, L., He, J., Wang, L., and Wang, Y., 2020. Local characteristics of and exposure to fine particulate matter ($PM_{2.5}$) in four indian megacities. *Atmospheric Environment: X*, *5*, 100052. https://doi.org/10.1016/j.aeaoa.2019.100052

Cheng, I., Zhang, L., Blanchard, P., Dalziel, J., and Tordon, R., 2013. Concentration-weighted trajectory approach to identifying potential sources of speciated atmospheric mercury at an urban coastal site in Nova Scotia, Canada. *Atmospheric Chemistry and Physics*, *13*(12), 6031–6048. https://doi.org/10.5194/acp-13-6031-2013

Chu, D. A., Ferrare, R., Szykman, J., Lewis, J., Scarino, A., Hains, J., Burton, S., Chen, G., Tsai, T., Hostetler, C., Hair, J., Holben, B., and Crawford, J., 2015. Regional characteristics of the relationship between columnar AOD and surface PM 2.5 : Application of lidar aerosol extinction profiles over Baltimore–Washington Corridor during DISCOVER-AQ. *Atmospheric Environment*, *101*, 338–349. https://doi.org/10.1016/j.atmosenv.2014.11.034

Conte, M., Merico, E., Cesari, D., Dinoi, A., Grasso, F. M., Donateo, A., Guascito, M. R., and Contini, D., 2020. Long-term characterisation of African dust advection in south-eastern Italy: Influence on fine and coarse particle concentrations, size distributions, and carbon content. *Atmospheric Research*, *233*, 104690. https://doi.org/10.1016/j.atmosres.2019.104690

Das, M., Das, A., Sarkar, R., Mandal, P., Saha, S., and Ghosh, S., 2021. Exploring short term spatio-temporal pattern of $PM_{2.5}$ and PM_{10} and their relationship with meteorological parameters during COVID-19 in Delhi. *Urban Climate*, *39*, 100944. https://doi.org/10.1016/j.uclim.2021.100944

Deb, S., and Sil, B. S., 2019. Climate change study for the meteorological variables in the Barak River basin in North-East India. *Urban Climate*, *30*, 100530. https://doi.org/10.1016/j.uclim.2019.100530

Draxler, R. R., and Hess, G. D., n.d.*NOAA Technical Memorandum ERL ARL-224*31.

Ferrero, L., Riccio, A., Ferrini, B. S., D'Angelo, L., Rovelli, G., Casati, M., Angelini, F., Barnaba, F., Gobbi, G. P., Cataldi, M., and Bolzacchini, E., 2019. Satellite AOD conversion into ground PM_{10}, $PM_{2.5}$ and PM1 over the Po valley (Milan, Italy) exploiting information on aerosol vertical profiles, chemistry,

hygroscopicity and meteorology. *Atmospheric Pollution Research*, *10*(6), 1895–1912. https://doi.org/10.1016/j.apr.2019.08.003

Gebhart, K. A., Schichtel, B. A., Malm, W. C., Barna, M. G., Rodriguez, M. A., and Collett, J. L., 2011. Back-trajectory-based source apportionment of airborne sulfur and nitrogen concentrations at Rocky Mountain National Park, Colorado, USA. *Atmospheric Environment*, *45*(3), 621–633. https://doi.org/10.1016/j.atmosenv.2010.10.035

Gopal, K. R., Obul Reddy, K. R., Balakrishnaiah, G., Arafath, S. Md., Kumar Reddy, N. S., Rao, T. C., Reddy, T. L., and Reddy, R. R., 2016. Regional trends of aerosol optical depth and their impact on cloud properties over Southern India using MODIS data. *Journal of Atmospheric and Solar-Terrestrial Physics*, *146*, 38–48. https://doi.org/10.1016/j.jastp.2016.05.005

Govender, P., and Sivakumar, V., 2020. Application of k-means and hierarchical clustering techniques for analysis of air pollution: A review (1980–2019). *Atmospheric Pollution Research*, *11*(1), 40–56. https://doi.org/10.1016/j.apr.2019.09.009

Gummeneni, S., Yusup, Y. B., Chavali, M., and Samadi, S. Z., 2011. Source apportionment of particulate matter in the ambient air of Hyderabad city, India. *Atmospheric Research*, *101*(3), 752–764. https://doi.org/10.1016/j.atmosres.2011.05.002

Gupta, P., and Follette-Cook, M., 2020. MODIS to VIIRS Transition for Air Quality Applications. NASA Applied Remote Sensing Training Program (ARSET). https://appliedsciences.nasa.gov/join-mission/training/english/arset-modis-viirs-transition-air-quality-applications

Guttikunda, S. K., and Aggarwal, R., 2009. Contribution of vehicular activity to air pollution in Hyderabad, India: Measurements, chemistry and analysis. *Indian Journal of Air Pollution Control*, *IX*(March), 37–46.

Han, Y. J., Holsen, T. M., and Hopke, P. K., 2007. Estimation of source locations of total gaseous mercury measured in New York State using trajectory-based models. *Atmospheric Environment*, *41*(28), 6033–6047. https://doi.org/10.1016/j.atmosenv.2007.03.027

Harrison, R. M., and Yin, J., 2000. Particulate matter in the atmosphere: which particle properties are important for its effects on health? *Science of The Total Environment*, *249*(1–3), 85–101. https://doi.org/10.1016/S0048-9697(99)00513-6

Hong, Q., Liu, C., Hu, Q., Xing, C., Tan, W., Liu, H., Huang, Y., Zhu, Y., Zhang, J., Geng, T., and Liu, J., 2019. Evolution of the vertical structure of air pollutants during winter heavy pollution episodes: The role of regional transport and potential sources. *Atmospheric Research*, *228*, 206–222. https://doi.org/10.1016/j.atmosres.2019.05.016

Ichoku, C., 2002. A spatio-temporal approach for global validation and analysis of MODIS aerosol products. *Geophysical Research Letters*, *29*(12), 8006. https://doi.org/10.1029/2001GL013206

Jain, S., Sharma, S. K., Srivastava, M. K., Chatterjee, A., Vijayan, N., Tripathy, S. S., Kumari, K. M., Mandal, T. K., and Sharma, C., 2021. Chemical characterization, source apportionment and transport pathways of $PM_{2.5}$ and PM_{10} over Indo Gangetic Plain of India. *Urban Climate*, *36*, 100805. https://doi.org/10.1016/j.uclim.2021.100805

Jeong, U., Kim, J., Lee, H., and Lee, Y. G., 2017. Assessing the effect of long-range pollutant transportation on air quality in Seoul using the conditional potential source contribution function method. *Atmospheric Environment*, *150*, 33–44. https://doi.org/10.1016/j.atmosenv.2016.11.017

Just, A. C., Wright, R. O., Schwartz, J., Coull, B. A., Baccarelli, A. A., Tellez-Rojo, M. M., Moody, E., Wang, Y., Lyapustin, A., and Kloog, I., 2015. Using High-Resolution Satellite Aerosol Optical Depth To Estimate Daily $PM_{2.5}$ Geographical Distribution in Mexico City. *Environmental Science and Technology*, *49*(14), 8576–8584. https://doi.org/10.1021/acs.est.5b00859

Kalaiarasan, G., Balakrishnan, R. M., Sethunath, N. A., and Manoharan, S., 2018. Source apportionment studies on particulate matter (PM_{10} and $PM_{2.5}$) in ambient air of urban Mangalore, India. *Journal of Environmental Management*, *217*, 815–824. https://doi.org/10.1016/j.jenvman.2018.04.040

Kaufman, Y. J., Remer, L. A., Tanre, D., Rong-Rong Li, Kleidman, R., Mattoo, S., Levy, R. C., Eck, T. F., Holben, B. N., Ichoku, C., Martins, J. V., and Koren, I., 2005. A critical examination of the residual cloud contamination and diurnal sampling effects on MODIS estimates of aerosol over ocean. *IEEE Transactions on Geoscience and Remote Sensing*, *43*(12), 2886–2897. https://doi.org/10.1109/TGRS.2005.858430

Kaufman, Y. J., and Tanré, D., 1998. *Algorithm for remote sensing of tropospheric aerosol from MODIS. NASA MODIS Algorithm Theoretical Basis Document*3–68.

Kharol, S. K., Badarinath, K. V. S., Sharma, A. R., Kaskaoutis, D. G., and Kambezidis, H. D., 2011. Multiyear analysis of Terra/Aqua MODIS aerosol optical depth and ground observations over tropical urban region of Hyderabad, India. *Atmospheric Environment*, *45*(8), 1532–1542. https://doi.org/10.1016/j.atmosenv.2010.12.047

Koelemeijer, R. B. A., Homan, C. D., and Matthijsen, J., 2006. Comparison of spatial and temporal variations of aerosol optical thickness and particulate matter over Europe. *Atmospheric Environment*, *40*(27), 5304–5315. https://doi.org/10.1016/j.atmosenv.2006.04.044

Kong, X., He, W., Qin, N., He, Q., Yang, B., Ouyang, H., Wang, Q., and Xu, F., 2013. Comparison of transport pathways and potential sources of PM_{10} in two cities around a large Chinese lake using the

modified trajectory analysis. *Atmospheric Research*, *122*, 284–297. https://doi.org/10.1016/j.atmosres.2012.10.012

Kumar, N., Chu, A., and Foster, A., 2008. Remote sensing of ambient particles in Delhi and its environs: estimation and validation. *International Journal of Remote Sensing*, *29*(12), 3383–3405. https://doi.org/10.1080/01431160701474545

Kumar, N., Jaswal, A. K., Mohapatra, M., and Kore, P. A., 2017. Spatial and temporal variation in daily temperature indices in summer and winter seasons over India (1969–2012). *Theoretical and Applied Climatology*, *129*(3–4), 1227–1239. https://doi.org/10.1007/s00704-016-1844-4

Kumar, S., Srivastava, A. K., Pathak, V., Bisht, D. S., and Tiwari, S., 2019. Surface solar radiation and its association with aerosol characteristics at an urban station in the Indo-Gangetic Basin: Implication to radiative effect. *Journal of Atmospheric and Solar-Terrestrial Physics*, *193*, 105061. https://doi.org/10.1016/j.jastp.2019.105061

Lee, H. J., Liu, Y., Coull, B. A., Schwartz, J., and Koutrakis, P., 2011. A novel calibration approach of MODIS AOD data to predict PMandlt;subandgt;2.5andlt;/subandgt; concentrations. *Atmospheric Chemistry and Physics*, *11*(15), 7991–8002. https://doi.org/10.5194/acp-11-7991-2011

Levy, R., and Hsu, C., et al., 2017. *MYD04_L2 MODIS/Aqua Aerosol 5-Min L2 Swath 10km* [Data set]NASA Level 1 and Atmosphere Archive and Distribution System. https://doi.org/10.5067/MODIS/MYD04_L2.061

Li, C., Dai, Z., Liu, X., and Wu, P., 2020. Transport Pathways and Potential Source Region Contributions of $PM_{2.5}$ in Weifang: Seasonal Variations. *Applied Sciences*, *10*(8), 2835. https://doi.org/10.3390/app10082835

Liao, T., Wang, S., Ai, J., Gui, K., Duan, B., Zhao, Q., Zhang, X., Jiang, W., and Sun, Y., 2017. Heavy pollution episodes, transport pathways and potential sources of $PM_{2.5}$ during the winter of 2013 in Chengdu (China). *Science of The Total Environment*, *584–585*, 1056–1065. https://doi.org/10.1016/j.scitotenv.2017.01.160

Liu, Y., Sarnat, J. A., Kilaru, V., Jacob, D. J., and Koutrakis, P., 2005. Estimating Ground-Level $PM_{2.5}$ in the Eastern United States Using Satellite Remote Sensing. *Environmental Science and Technology*, *39*(9), 3269–3278. https://doi.org/10.1021/es049352m

Ma, T., Duan, F., He, K., Qin, Y., Tong, D., Geng, G., Liu, X., Li, H., Yang, S., Ye, S., Xu, B., Zhang, Q., and Ma, Y., 2019. Air pollution characteristics and their relationship with emissions and meteorology in the Yangtze River Delta region during 2014–2016. *Journal of Environmental Sciences*, *83*, 8–20. https://doi.org/10.1016/j.jes.2019.02.031

Ma, Z., Hu, X., Huang, L., Bi, J., and Liu, Y., 2014. Estimating Ground-Level PM $_{2.5}$ in China Using Satellite Remote Sensing. *Environmental Science and Technology*, *48*(13), 7436–7444. https://doi.org/10.1021/es5009399

Mahapatra, P. S., Sinha, P. R., Boopathy, R., Das, T., Mohanty, S., Sahu, S. C., and Gurjar, B. R., 2018. Seasonal progression of atmospheric particulate matter over an urban coastal region in peninsular India: Role of local meteorology and long-range transport. *Atmospheric Research*, *199*, 145–158. https://doi.org/10.1016/j.atmosres.2017.09.001

Munchak, L. A., Levy, R. C., Mattoo, S., Remer, L. A., Holben, B. N., Schafer, J. S., Hostetler, C. A., and Ferrare, R. A., 2013. MODIS 3 km aerosol product: applications over land in an urban/suburban region. *Atmospheric Measurement Techniques*, *6*(7), 1747–1759. https://doi.org/10.5194/amt-6-1747-2013

Newman, J. D., Bhatt, D. L., Rajagopalan, S., Balmes, J. R., Brauer, M., Breysse, P. N., Brown, A. G. M., Carnethon, M. R., Cascio, W. E., Collman, G. W., Fine, L. J., Hansel, N. N., Hernandez, A., Hochman, J. S., Jerrett, M., Joubert, B. R., Kaufman, J. D., Malik, A. O., Mensah, G. A., … Brook, R. D., 2020. Cardiopulmonary Impact of Particulate Air Pollution in High-Risk Populations. *Journal of the American College of Cardiology*, *76*(24), 2878–2894. https://doi.org/10.1016/j.jacc.2020.10.020

Pandey, A., Brauer, M., Cropper, M. L., Balakrishnan, K., Mathur, P., Dey, S., Turkgulu, B., Kumar, G. A., Khare, M., Beig, G., Gupta, T., Krishnankutty, R. P., Causey, K., Cohen, A. J., Bhargava, S., Aggarwal, A. N., Agrawal, A., Awasthi, S., Bennitt, F., … Dandona, L., 2021. Health and economic impact of air pollution in the states of India: the Global Burden of Disease Study 2019. *The Lancet Planetary Health*, *5*(1), e25–e38. https://doi.org/10.1016/S2542-5196(20)30298-9

Pani, S. K., and Verma, S., 2014. Variability of winter and summertime aerosols over eastern India urban environment. *Atmospheric Research*, *137*, 112–124. https://doi.org/10.1016/j.atmosres.2013.09.014

Pant, P., Guttikunda, S. K., and Peltier, R. E., 2016. Exposure to particulate matter in India: A synthesis of findings and future directions. *Environmental Research*, *147*, 480–496. https://doi.org/10.1016/j.envres.2016.03.011

Pant, P., and Harrison, R. M., 2012. Critical review of receptor modelling for particulate matter: A case study of India. *Atmospheric Environment*, *49*, 1–12. https://doi.org/10.1016/j.atmosenv.2011.11.060

Park, S., Lee, J., Im, J., Song, C.-K., Choi, M., Kim, J., Lee, S., Park, R., Kim, S.-M., Yoon, J., Lee, D.-W., and Quackenbush, L. J., 2020. Estimation of spatially continuous daytime particulate matter concentrations under all sky conditions through the synergistic use of satellite-based AOD and

numerical models. *Science of The Total Environment*, *713*, 136516. https://doi.org/10.1016/j.scitotenv.2020.136516

Raaschou-Nielsen, O., Beelen, R., Wang, M., Hoek, G., Andersen, Z. J., Hoffmann, B., Stafoggia, M., Samoli, E., Weinmayr, G., Dimakopoulou, K., Nieuwenhuijsen, M., Xun, W. W., Fischer, P., Eriksen, K. T., Sørensen, M., Tjønneland, A., Ricceri, F., de Hoogh, K., Key, T., … Vineis, P., 2016. Particulate matter air pollution components and risk for lung cancer. *Environment International*, *87*, 66–73. https://doi.org/10.1016/j.envint.2015.11.007

Ramachandran, S., 2005. PM mass concentrations in comparison with aerosol optical depths over the Arabian Sea and Indian Ocean during winter monsoon. *Atmospheric Environment*, *39*(10), 1879–1890. https://doi.org/10.1016/j.atmosenv.2004.12.003

Ramachandran, S., Kedia, S., and Srivastava, R., 2012. Aerosol optical depth trends over different regions of India. *Atmospheric Environment*, *49*, 338–347. https://doi.org/10.1016/j.atmosenv.2011.11.017

Ravindra, K., Rattan, P., Mor, S., and Aggarwal, A. N., 2019. Generalized additive models: Building evidence of air pollution, climate change and human health. *Environment International*, *132*, 104987. https://doi.org/10.1016/j.envint.2019.104987

Remer, L. A., Kaufman, Y. J., Tanré, D., Mattoo, S., Chu, D. A., Martins, J. V., Li, R.-R., Ichoku, C., Levy, R. C., Kleidman, R. G., Eck, T. F., Vermote, E., and Holben, B. N., 2005. aThe MODIS Aerosol Algorithm, Products, and Validation. *Journal of the Atmospheric Sciences*, *62*(4), 947–973. https://doi.org/10.1175/JAS3385.1

Remer, L. A., Kaufman, Y. J., Tanré, D., Mattoo, S., Chu, D. A., Martins, J. V., Li, R.-R., Ichoku, C., Levy, R. C., Kleidman, R. G., Eck, T. F., Vermote, E., and Holben, B. N., 2005. bThe MODIS Aerosol Algorithm, Products, and Validation. *Journal of the Atmospheric Sciences*, *62*(4), 947–973. https://doi.org/10.1175/JAS3385.1

Sathe, Y., Kulkarni, S., Gupta, P., Kaginalkar, A., Islam, S., and Gargava, P., 2019. Application of Moderate Resolution Imaging Spectroradiometer (MODIS) Aerosol Optical Depth (AOD) and Weather Research Forecasting (WRF) model meteorological data for assessment of fine particulate matter ($PM_{2.5}$) over India. *Atmospheric Pollution Research*, *10*(2), 418–434. https://doi.org/10.1016/j.apr.2018.08.016

Seibert, P., Kromp-Kolb, H., Baltensperger, U., Jost, D. T., and Schwikowski, M., 1994. Trajectory Analysis of High-Alpine Air Pollution Data. In S.-E. Gryning and M. M. Millán (Eds.), *Air Pollution Modeling and Its Application X* (pp. 595–596)Springer US. https://doi.org/10.1007/978-1-4615-1817-4_65

Shaik, D. S., Kant, Y., Mitra, D., Singh, A., Chandola, H. C., Sateesh, M., Babu, S. S., and Chauhan, P., 2019. Impact of biomass burning on regional aerosol optical properties: A case study over northern India. *Journal of Environmental Management*, *244*, 328–343. https://doi.org/10.1016/j.jenvman.2019.04.025

Shao, P., Xin, J., An, J., Kong, L., Wang, B., Wang, J., Wang, Y., and Wu, D., 2017. The empirical relationship between $PM_{2.5}$ and AOD in Nanjing of the Yangtze River Delta. *Atmospheric Pollution Research*, *8*(2), 233–243. https://doi.org/10.1016/j.apr.2016.09.001

Sharma, M., and Maloo, S., 2005. Assessment of ambient air PM and PM and characterization of PM in the city of Kanpur, India. *Atmospheric Environment*, *39*(33), 6015–6026. https://doi.org/10.1016/j.atmosenv.2005.04.041

Shie, R.-H., and Chan, C.-C., 2013. Tracking hazardous air pollutants from a refinery fire by applying on-line and off-line air monitoring and back trajectory modeling. *Journal of Hazardous Materials*, *261*, 72–82. https://doi.org/10.1016/j.jhazmat.2013.07.017

Soni, M., Payra, S., and Verma, S., 2018. Particulate matter estimation over a semi arid region Jaipur, India using satellite AOD and meteorological parameters. *Atmospheric Pollution Research*, *9*(5), 949–958. https://doi.org/10.1016/j.apr.2018.03.001

Sun, J., Zhang, M., and Liu, T., 2001. Spatial and temporal characteristics of dust storms in China and its surrounding regions, 1960-1999: Relations to source area and climate. *Journal of Geophysical Research: Atmospheres*, *106*(D10), 10325–10333. https://doi.org/10.1029/2000JD900665

Tian, J., and Chen, D., 2010. A semi-empirical model for predicting hourly ground-level fine particulate matter ($PM_{2.5}$) concentration in southern Ontario from satellite remote sensing and ground-based meteorological measurements. *Remote Sensing of Environment*, *114*(2), 221–229. https://doi.org/10.1016/j.rse.2009.09.011

Tiwari, S., Pandithurai, G., Attri, S. D., Srivastava, A. K., Soni, V. K., Bisht, D. S., Anil Kumar, V., and Srivastava, M. K., 2015. Aerosol optical properties and their relationship with meteorological parameters during wintertime in Delhi, India. *Atmospheric Research*, *153*, 465–479. https://doi.org/10.1016/j.atmosres.2014.10.003

Tuna Tuygun, G., Gündoğdu, S., and Elbir, T., 2021. Estimation of ground-level particulate matter concentrations based on synergistic use of MODIS, MERRA-2 and AERONET AODs over a coastal site in the Eastern Mediterranean. *Atmospheric Environment*, *261*, 118562. https://doi.org/10.1016/j.atmosenv.2021.118562

Wang, Q., Zeng, Q., Tao, J., Sun, L., Zhang, L., Gu, T., Wang, Z., and Chen, L., 2019. Estimating $PM_{2.5}$ Concentrations Based on MODIS AOD and NAQPMS Data over Beijing–Tianjin–Hebei. *Sensors*, *19*(5), 1207. https://doi.org/10.3390/s19051207

Wang, Y. Q., 2014. MeteoInfo: GIS software for meteorological data visualization and analysis: Meteorological GIS software. *Meteorological Applications*, *21*(2), 360–368. https://doi.org/10.1002/met.1345

Wang, Y. Q., Zhang, X. Y., and Arimoto, R., 2006. The contribution from distant dust sources to the atmospheric particulate matter loadings at XiAn, China during spring. *Science of The Total Environment*, *368*(2–3), 875–883. https://doi.org/10.1016/j.scitotenv.2006.03.040

Wang, Y. Q., Zhang, X. Y., and Draxler, R. R., 2009. TrajStat: GIS-based software that uses various trajectory statistical analysis methods to identify potential sources from long-term air pollution measurement data. *Environmental Modelling and Software*, *24*(8), 938–939. https://doi.org/10.1016/j.envsoft.2009.01.004

Yadav, R., Sahu, L. K., Beig, G., and Jaaffrey, S. N. A., 2016. Role of long-range transport and local meteorology in seasonal variation of surface ozone and its precursors at an urban site in India. *Atmospheric Research*, *176–177*, 96–107. https://doi.org/10.1016/j.atmosres.2016.02.018

Yadav, R., Sahu, L. K., Beig, G., Tripathi, N., Maji, S., and Jaaffrey, S. N. A., 2019. The role of local meteorology on ambient particulate and gaseous species at an urban site of western India. *Urban Climate*, *28*, 100449. https://doi.org/10.1016/j.uclim.2019.01.003

Yang, Q., Yuan, Q., Yue, L., Li, T., Shen, H., and Zhang, L., 2019. The relationships between $PM_{2.5}$ and aerosol optical depth (AOD) in mainland China: About and behind the spatio-temporal variations. *Environmental Pollution*, *248*, 526–535. https://doi.org/10.1016/j.envpol.2019.02.071

Yap, X. Q., and Hashim, M., 2013. A robust calibration approach for PMandlt;subandgt;10andlt;/subandgt; prediction from MODIS aerosol optical depth. *Atmospheric Chemistry and Physics*, *13*(6), 3517–3526. https://doi.org/10.5194/acp-13-3517-2013

Ying, Q., Mysliwiec, M., and Kleeman, M. J., 2004. Source Apportionment of Visibility Impairment Using a Three-Dimensional Source-Oriented Air Quality Model. *Environmental Science and Technology*, *38*(4), 1089–1101. https://doi.org/10.1021/es0349305

You, W., Zang, Z., Zhang, L., Li, Z., Chen, D., and Zhang, G., 2015. Estimating ground-level PM_{10} concentration in northwestern China using geographically weighted regression based on satellite AOD combined with CALIPSO and MODIS fire count. *Remote Sensing of Environment*, *168*, 276–285. https://doi.org/10.1016/j.rse.2015.07.020

Zhang, Y., Cai, J., Wang, S., He, K., and Zheng, M., 2017. Review of receptor-based source apportionment research of fine particulate matter and its challenges in China. *Science of The Total Environment, 586*, 917–929. https://doi.org/10.1016/j.scitotenv.2017.02.071

Zhang, Z. Y., Wong, M. S., and Lee, K. H., 2015. Estimation of potential source regions of PM 2.5 in Beijing using backward trajectories. *Atmospheric Pollution Research, 6*(1), 173–177. https://doi.org/10.5094/APR.2015.020

Appendix

Table A1. Model performance statistical parameters

	Parameter	Bollaram	Central University	IDA	Patancher	Sanathnagar	Zoo park
MOD_3K	RMSE	15	15	11	54	10	12
	D	0.53	0.59	0.81	0.21	0.78	0.76
	NMB	-0.15	-0.02	-0.02	-0.84	-0.04	0.05
	R	0.37	0.36	0.73	-0.43	0.69	0.6
MOD_L2	RMSE	12	14	12	55	11	11
	D	0.52	0.66	0.71	0.22	0.73	0.85
	NMB	-0.009	0.11	-0.03	-0.87	-0.03	0.1
	R	0.59	0.55	0.68	-0.39	0.62	0.8
MYOD_3K	RMSE	15	15	13	47	10	10
	D	0.52	0.73	0.62	0.25	0.81	0.74
	NMB	-0.12	0.14	-0.08	-0.67	-0.02	0.01
	R	0.53	0.62	0.72	-0.34	0.75	0.58
MYOD_L2	RMSE	14	16	11	44	11	11
	D	0.52	0.6	0.82	0.22	0.74	0.8
	NMB	-0.12	0.11	-0.04	-0.67	-0.01	0.09
	R	0.46	0.4	0.77	-0.5	0.65	0.75

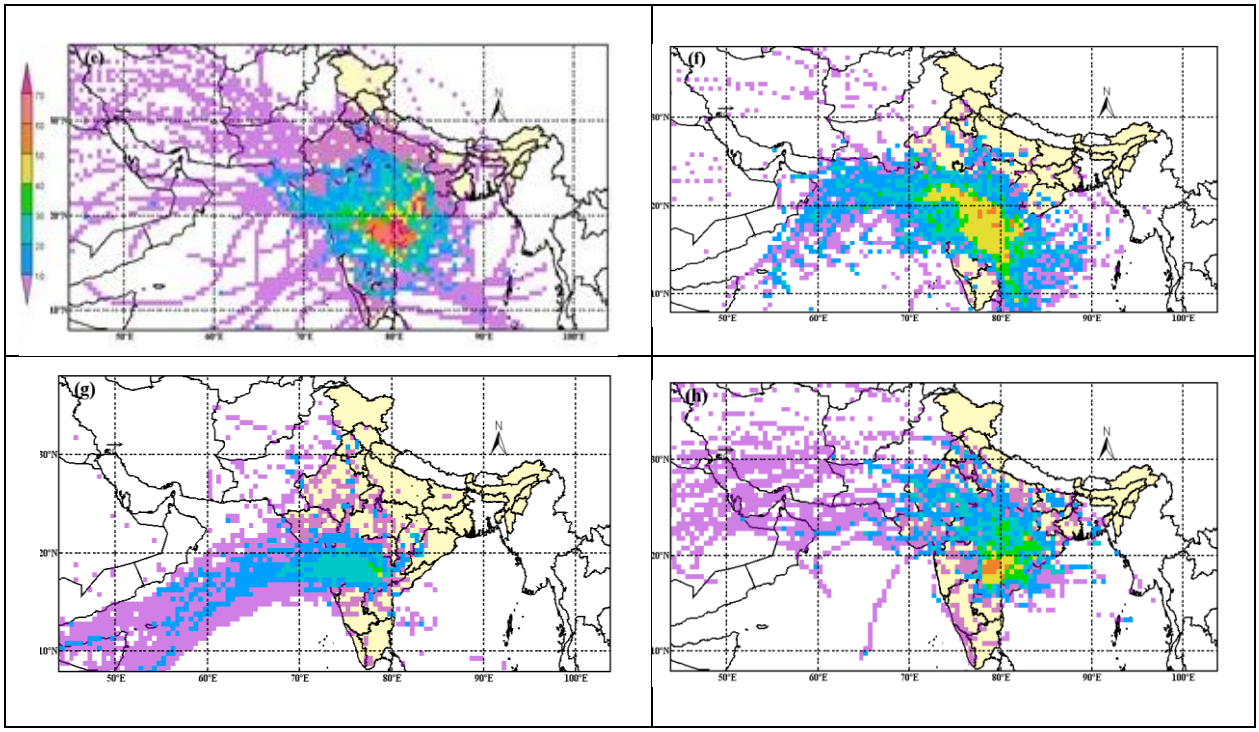

Fig. A1. CWT analysis with different seasons at elevated layer

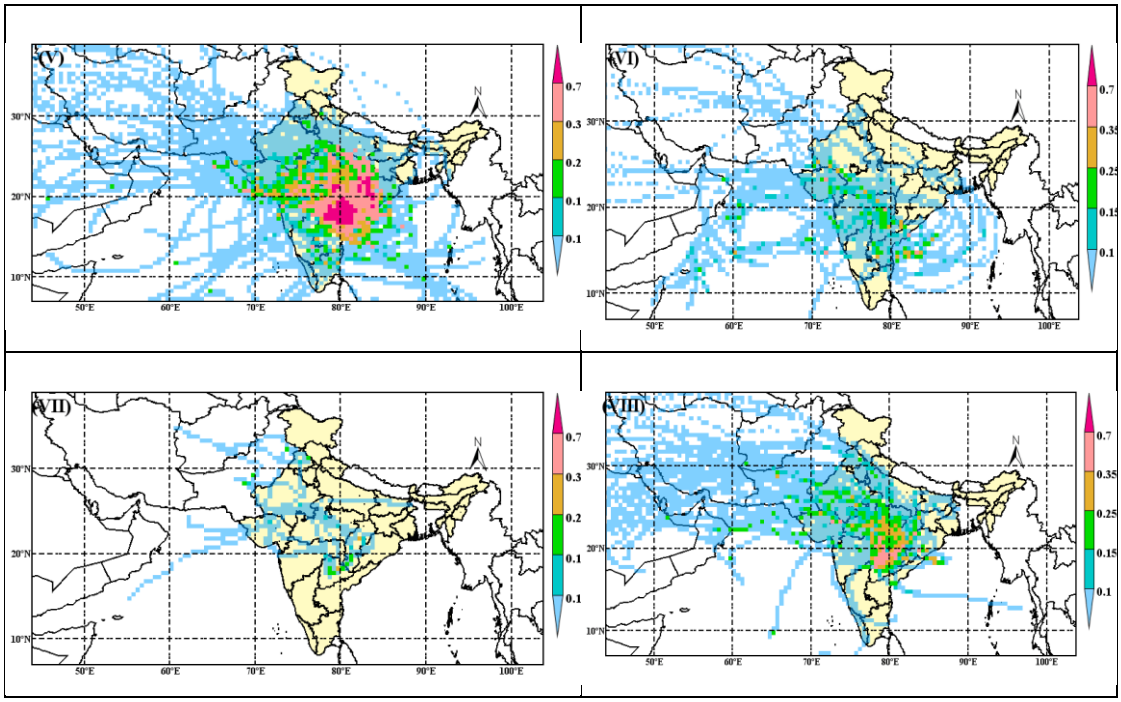

Fig. A2. PSCF analysis with different seasons at elevated layer

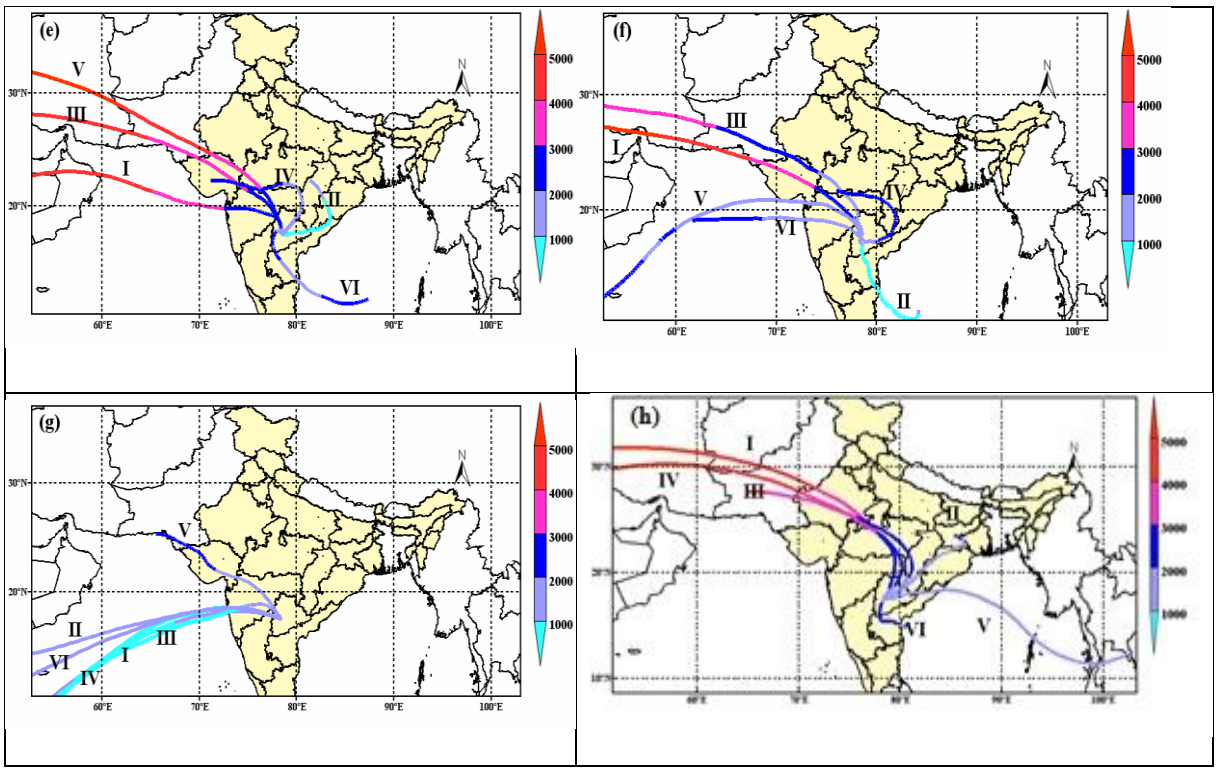

Fig. A3. Cluster analysis with different seasons at elevated layer

Table A2. Polluted clusters and associated trajectory's numbers at surface layer

Winter _sl	Number_traj	Mean_value	Standard deviation	Polluted_num	Polluted_mean_value	Polluted_stdev	Ratio(%)
1	202	72.05	8.43	179	74.52	4.83	21.6
2	45	65.21	11.61	29	72.81	5.75	8.33
3	79	68.07	1031	61	72.65	5.78	38.1
4	163	64.46	12.43	98	73.33	5.55	13.52
5	42	63.71	14.23	26	73.4	5.29	7.22
Pre_monsoon							
1	118	43.85	7.96	0	0	0	18.29
2	49	48.85	10.7	6	69.44	7.18	7.91
3	51	50.71	10.54	9	66.14	4	7.91
4	199	48.42	11.73	38	66.79	4.4	31.3
5	115	42.25	11.75	11	67.88	7.37	19.22
6	98	47.53	9.57	11	66.37	5.69	15.3
monsoon							
1	154	21.9	5.16	0	0	0	22.59
2	89	25.93	7.04	0	0	0	12.4
3	111	34.64	12.9	10	62.54	2.57	17.15
4	124	18.9	3.62	0	0	0	18.9
5	133	21.75	4.92	0	0	0	20.9
6	55	32.85	9.82	2	63.91	4.78	7.95
Post monsoon							
1	97	55.11	19.22	42	71.21	6.44	29.23
2	60	50.37	23.19	24	70.21	5.04	17.76
3	55	40.79	13.32	4	67.08	5.91	15.03
4	26	54.95	25.27	15	72.26	5.41	8.2
5	67	42.98	22.13	16	69.31	6.21	22.4
6	16	33.33	27.28	4	72.18	7.53	7.38

Table A3. Polluted clusters and associated trajectory's numbers at Elevated layer

Winter _el	Number _traj	Mean _value	Standard deviation	Polluted _num	Polluted _mean_value	Polluted_stdev	Ratio(%)
1	35	67.31	9.93	24	72.89	6.13	18.6
2	43	71.09	7.92	39	73.1	4.8	9
3	23	64.09	11.09	16	70.01	7.03	12.6
4	57	68.8	9.5	44	73.17	4.8	57
5	7	66.85	1.89	5	72.67	5.19	3.54
6	29	68.26	10	19	74.68	4.7	14.65
Pre monsoon							
1	38	50.95	10.7	8	65.81	2.95	9.30
2	101	46.1	10.18	10	67.1	6.06	23.72

3	47	46.78	10.8	6	69.95	6	10.93
4	72	48.33	10.31	8	67.03	4.56	16.74
5	51	48.51	11.8	7	67.56	8.56	12.09
6	111	44.94	10.99	11	65.99	3.4	27.21
Monsoon							
1	105	19.18	3.84	0	0	0	22.75
2	70	22.77	5.92	0	0	0	17.62
3	50	3.89	10.25	0	0	0	10.25
4	96	23.99	6.58	0	0	0	19.67
5	104	30.53	12.6	8	62.77	2.85	23.16
6	29	21.03	4.15	0	0	0	6.56
Post monsoon							
1	26	56.38	24.59	16	72.17	5.57	13.1
2	36	38.56	21.38	5	70.59	7.19	17.2
3	45	45.27	20.89	12	68.1	6.56	21.3
4	58	58.26	20.08	33	71.54	5.75	25
5	21	44.42	15.59	1	74.2	0	8.61
6	28	39.25	17.67	3	69	7.82	14.75

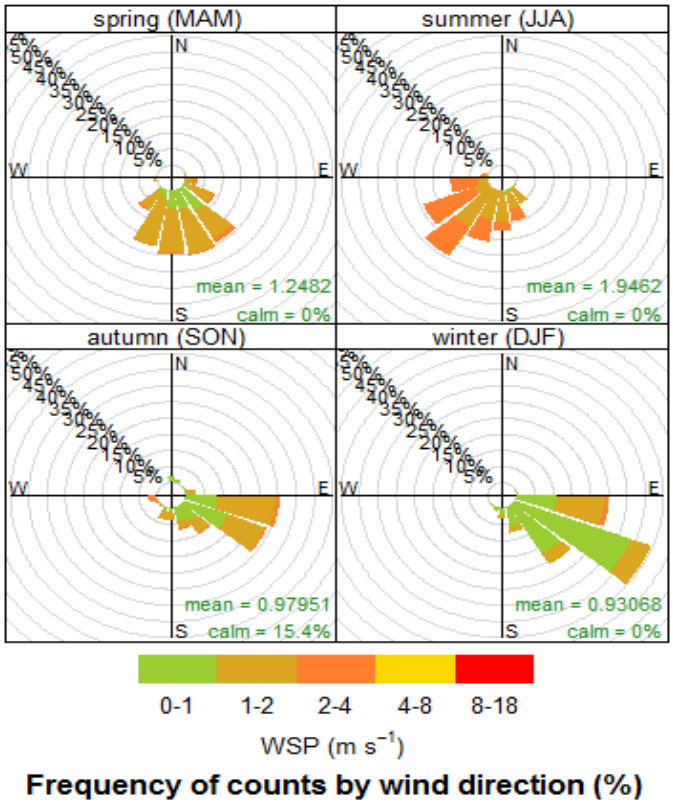

Fig. A4. Sanathnagar wind rose diagram for all seasons

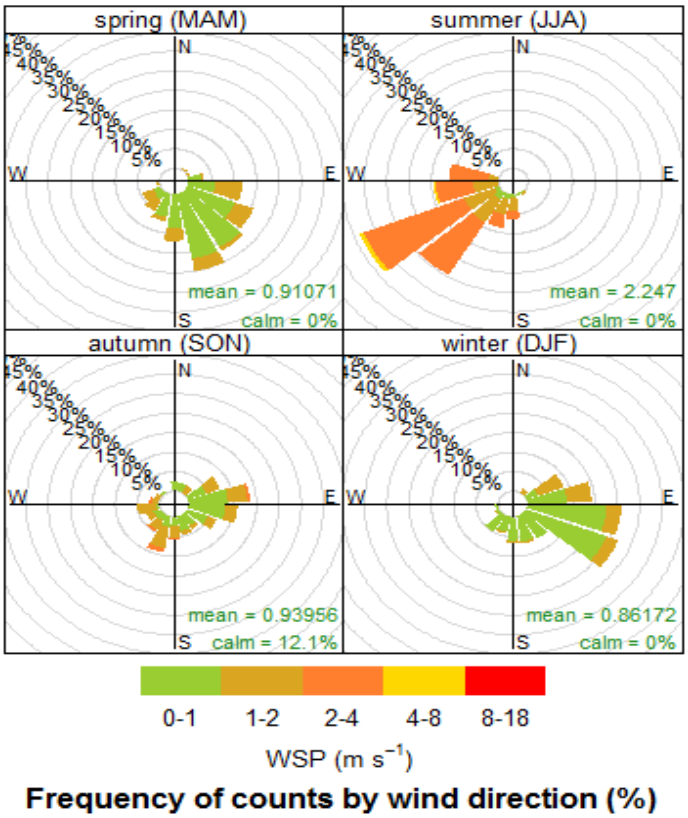

Fig. A5. Patancher wind rose diagram for all seasons

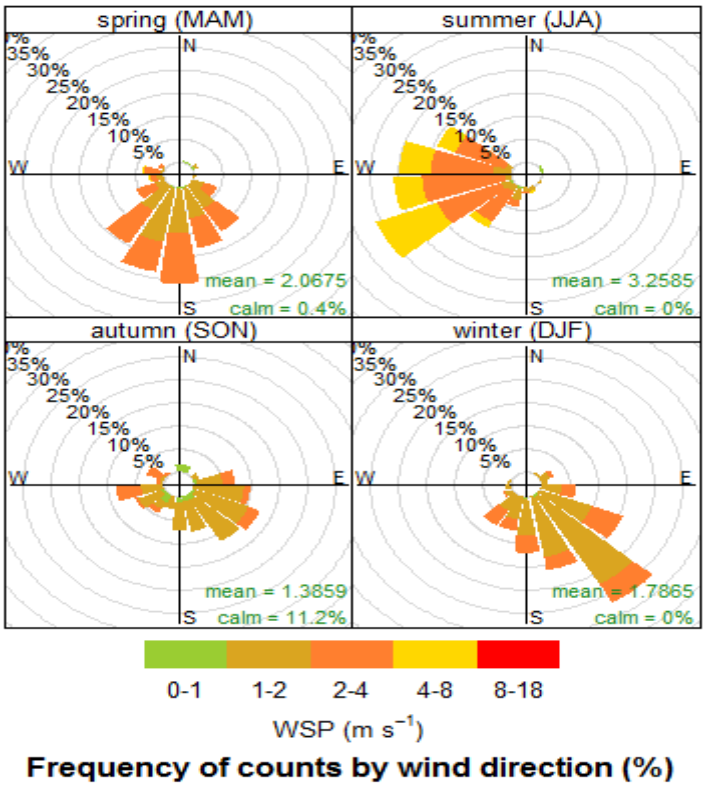

Fig. A6. IDA wind rose diagram for all seasons

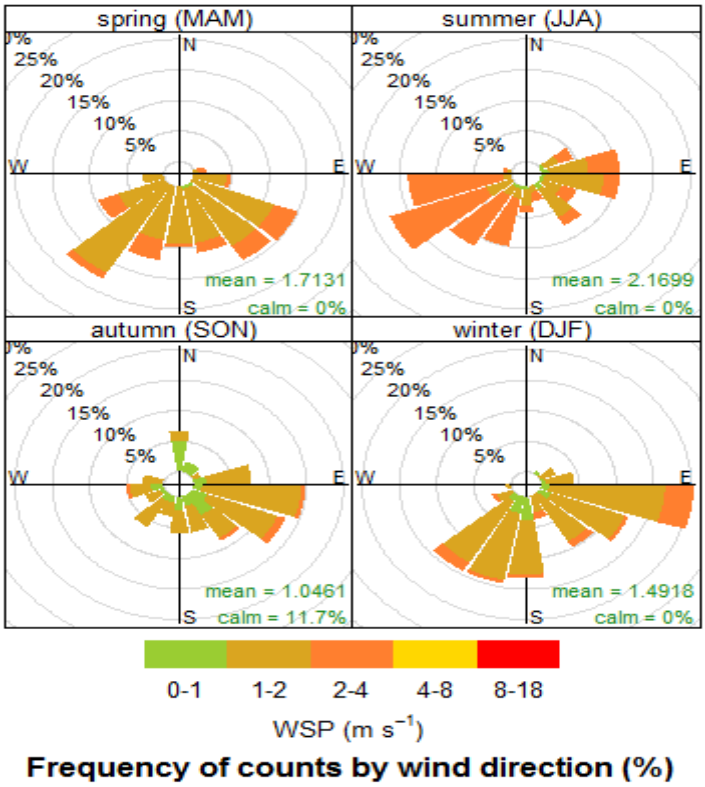

Fig. A7. CU wind rose diagram for all seasons

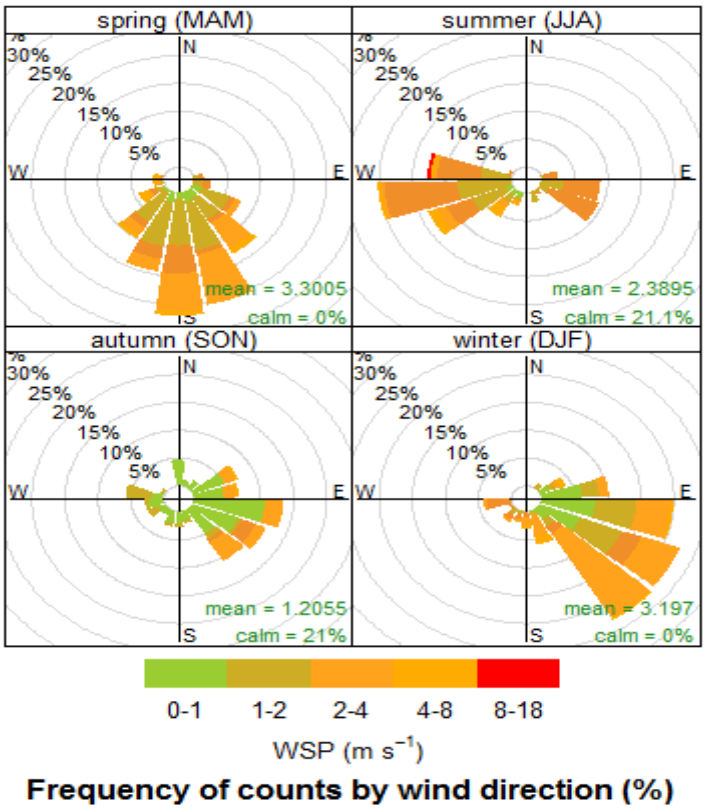

Fig. A8. Bollaram wind rose diagram for all seasons